On the Single-Doppler Measurements of Divergence in Clear Air

R. RABIN AND I. ZAWADZKI[1]

National Severe Storms Laboratory, Norman, OK 73069

(Manuscript received 14 July 1983, in final form 15 December 1983)

ABSTRACT

The relationship between convective scales in the pre-storm environment and Doppler measurements of divergence is discussed with attention to problems inherent in radar measurements. A method is suggested to minimize the effects of beam smoothing and reflectivity weighting. A case study indicates the possibility of operational short-term forecasting of the onset time of precipitation from the radar measurements of divergence.

1. Introduction

The possibility of obtaining the kinematic properties of airflow from single-Doppler radar observations has been of interest for a number of years. In an early work, Browning and Wexler (1968) have shown that harmonic analysis of the azimuthal Doppler velocity field can yield, under the assumption of linearity of the flow, the mean wind speed and direction, and the mean deformation over a circle with the radar at its center. Also, the mean divergence can be obtained directly without the linearity assumption (for sufficiently sampled and evenly spaced data). This technique, known as velocity-azimuth display (VAD), is probably the most accepted way of analyzing single-Doppler data.

Based also on the assumption of linearity of the velocity field, Easterbrook (1975) proposed an extension of the VAD technique by which fields of divergence could be obtained. This idea was further developed by Waldteufel and Corbin (1979) who applied it to three-dimensional observations (volume velocity processing, VVP). Additional refinements were introduced by Koscielny *et al.* (1982).

The obvious limitation to the approach represented by the works mentioned above is the validity of the linear approximation to the air flow. In convective situations the various cells of vertical motion are associated with a highly variable field of divergence. The measurements from a high-density network of anemometers reported by Ulanski and Garstang (1978) illustrate well this point: over a distance of 10 km the horizontal divergence varies by a factor of 2 and the lines of constant divergence have a tendency to circularity, that is, indicating strong nonlinearities. It is likely that such nonlinear aspects of the flow are the most significant in relation to clear air convection just prior to storm development and limit the usefulness of techniques based on the linear wind assumption, such as VVP.

The purpose of the present work is to analyze the meaning of the only measurement by a single-Doppler radar which is quite accurate and independent of any assumption, that is, the average divergence as obtained by the simple azimuth average of the radial velocity (at low elevations) and to explore the possible operational applications of these measurements in the pre-storm environment.

2. Doppler radar measurements in clear air

In polar coordinates with the origin at the radar site, Doppler radar measures the radial velocity component of whatever backscatters sufficient energy to be detectable: clouds, birds, variation in refractive index, etc. Consequently, velocity measurements in clear air have to be carefully edited to eliminate spurious and noisy values. This can be done using two criteria: 1) a lower limit for the covariance of signal plus noise which systematically decreases as the echo signal weakens thus indicating a poorer velocity estimate and 2) an upper limit for echo intensity which eliminates velocities due to highly reflecting objects such as aircraft, birds, etc. After the editing is done, what is left represents typically ~70% of the radial velocity measurements at unequally spaced azimuths. Rabin and Zrnic' (1980) have developed a technique for VAD analysis of data at unequally spaced azimuths. When the velocity measurements are integrated over 360° in azimuth, the flux of the vector velocity out of the circle of radius r (where r is the range at which the azimuth integration is performed) is obtained. For low antenna elevation angles, the Doppler velocity is essentially the radial component v_r of the horizontal

[1] Permanent affiliation: Universite du Quebec a Montreal, Canada. Visiting Research Fellow at the Cooperative Institute for Mesoscale Meteorological Studies.

velocity and by virtue of Green's theorem, the measured flux equals the average horizontal divergence over the circle of radius r. The average horizontal divergence is the only kinematic wind property determined by a single Doppler which can be independent of any assumptions about the air flow. Although the measurement errors in v_r are of the order of 1 m s^{-1} over circles between ranges of 40–90 km, the error in the average horizontal divergence is of the orderof 10^{-5} to 10^{-6} s^{-1}. Consequently, there is a definite motivation to exploit these measurements as much as possible.

3. Scales associated with radar measured divergence

At the early stage of the pre-storm environment we might expect that the divergence field will have mainly small-scale variability such as in Fig. 1a. Such situations are revealed occasionally by a sky partially covered by small cumuli. With increasing available convective energy, the horizontal divergence will tend to organize into larger and more intense convective elements as in Fig. 1b. A diagram showing the average horizontal divergence $\bar{D}(r)$ over a circle of radius r as a function of r should reveal a large variability of $\bar{D}$ for r comparable to the convective scales present in the environment. As r increases to encompass more and more convective eddys, the field of divergence is increasingly smoothed and the function $\bar{D}(r)$ will show decreasing variability with range. With increasing size of the convective elements, the radius at which $\bar{D}$ becomes nearly uniform in range should increase. Fig. 1 represents schematically this situation.

Actually the measured $\bar{D}(r)$ may contain divergence from a wide range of scales. The filtering response may be obtained by following Stevens (1967) who showed that $\bar{D}(r)$ is equivalent to averaging divergence inside a circle of radius r. Thus, we have uniform weighting of divergence over all ranges between zero and r. The power transfer function of $\bar{D}(r)$ is given by

$$\frac{\bar{P}(k)}{P(k)} = 4\left[\frac{J_1(kr)}{kr}\right], \tag{1}$$

where P is the spectral density of divergence as a function of the two-dimensional wavenumber k, $\bar{P}$ is the spectral density after filtering with $\bar{D}(r)$ and J_1 is a Bessel function of the first kind and order 1. The power transfer function of $\bar{D}(r)$ is plotted as a function of L/r (where L is wavelength) in Fig. 2. Scales less than $2r$ are nearly completely attenuated, while wavelengths of $10r$ and greater are virtually unattenuated. The larger scale fields should appear horizontally uniform over the entire area observed by the radar. Thus $\bar{D}(r)$ in Fig. 1 may include a constant value representing the subsynoptic divergence D_s. Although in the horizontal dimension D_s will appear quite uniform within the radar observed distances, its vertical structure could be quite varied.

On the other hand, radar samples are never obtained at a constant altitude; even for a zero elevation angle of the antenna, the earth curvature introduces a certain vertical distance z between the height of the radar observation and the earth's surface (at r = 100 km, z = 600 m). An elevation angle θ of 1° makes z = 2340 m at r = 100 km. Thus, over the range of 100 km the radar beam sweeps through the entire boundary layer. The vertical variation of D_s contributes to the change of $\bar{D}(r)$ with range. In this way the vertical variation of the subsynoptic scale of divergence is detected by the radar and added to the convective scales.

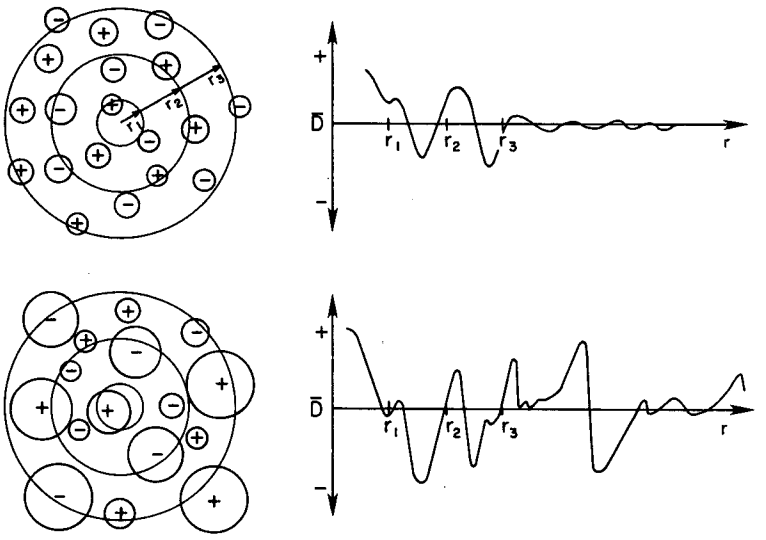

FIG. 1. Schematic illustration of the relationship between the convective scales of upward [+] and downward [−] motion and the range variation of the average horizontal divergence.

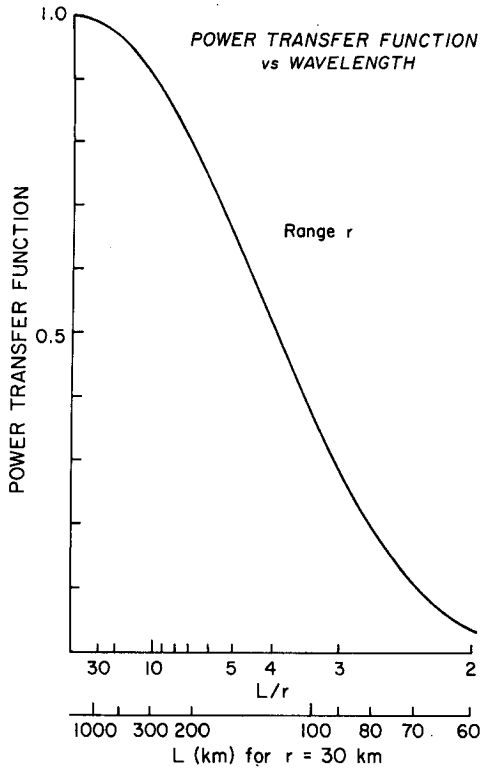

FIG. 2. Power transfer function versus wavelength for measurement of divergence at a given range r.

4. Radar beam averaging

Increasing beamwidth with range introduces a range-dependent smoothing, with the result that the detected average divergence will show the range variability of $\bar{D}$ decreasing with range more rapidly than it actually occurs in nature. Both the subsynoptic and the smaller scales are affected by the beam smoothing. Fig. 3 is an example of actual measurements of $\bar{D}(r)$ at an early stage of the pre-storm environment. Due to the presence of ground clutter for $r < 30$ km, $\bar{D}$ is not shown for the short ranges. All the features discussed so far can be observed on this diagram: the large-scale oscillation of $\bar{D}$, going from divergence to convergence and to divergence again, is probably indicative of the large-scale vertical variation of divergence over a depth of 1.4 km. The range decreasing amplitude of this oscillation is due to averaging more eddies over the increasing area, and also to the beam smoothing as it increases with range. The smaller scale variability of $\bar{D}$ is more pronounced at short ranges due to both the smaller averaging area and less beam smoothing. The close resemblance of the two curves reinforces the confidence in the accuracy of the measurements.

We will now formulate mathematically the radar measurements of divergence $\bar{D}$. For simplicity, it will be assumed that the Doppler velocities are available at evenly spaced azimuths (ϕ) and measured at small elevation angles θ: $v_r(\phi, r, z)$ will denote the actual radial component of the air velocity; and the radar measured velocity $v_0(\phi, r, z)$ depends on v_r and the distribution of reflectivity η within the radar resolution volume. The transformation from v_r to v_0 is made by the smoothing of the reflectivity-weighted radial velocity with the resolution volume weighting function.

This weighting function will be denoted here by $W = W_1 W_2 W_3$, where each factor represents the azimuth, height and range, respectively, of the two-way beam pattern and range-weighting function (Doviak and Zrnic', 1978). These functions will be assumed normalized so that

$$\int_{\infty}^{\infty} W_j dX_j = 1, \quad j = 1, 2, 3; \quad X_j = \phi, r, z. \tag{2}$$

The radar measurements can be seen as samples of the convolution of W with reflectivity-weighted radial velocity. Thus, the measured mean radial velocity is

$$v_0(\phi_i, r, z) = \frac{1}{B_i} \int_{-\infty}^{\infty'} \int_{-\infty}^{r} \int_{0}^{2\pi} \eta(\phi_i - \phi', r - r', z - z') \times v_r(\phi_i - \phi', r - r', z - z') \times W(\phi', r', z') r' d\phi' dr' dz', \tag{3}$$

where ϕ_i, r and z are the azimuth, range and height of the resolution volume center with respect to the radar and primes indicate deviations from the center; B_i is the resolution volume-weighted reflectivity, i.e.,

$$B_i = \int_{-\infty}^{\infty} \int_{-\infty}^{r} \int_{0}^{2\pi} \eta(\phi_i - \phi', r - r', z - z') \times W(\phi', r', z') r' d\phi' dr' dz'. \tag{4}$$

Because the range weighting function at distances where divergence measurements are made is much narrower than the beam weighting function, we will ignore its smoothing. Consequently, the triple integrals in (3) and (4) reduce to double integrals (along z and ϕ). For example,

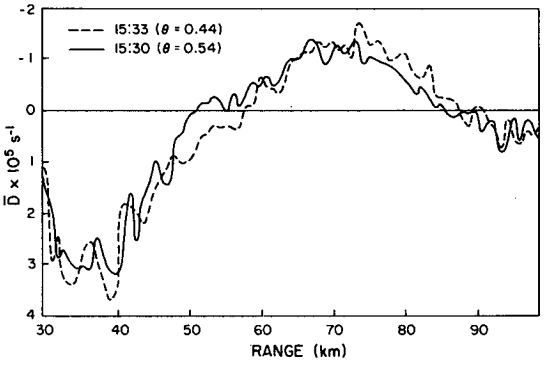

FIG. 3. An example of two measurements of average horizontal divergence at two close elevations and times.

$$B_i = r'B_i'$$

$$= r' \int_{-\infty}^{\infty} \int_0^{2\pi} \eta(\phi_i - \phi', z - z') W(\phi', z') d\phi' dz'. \quad (4')$$

From the "normal" vector form of Green's theorem (Thomas, 1968, p. 604), the radar-measured average divergence (not the true divergence) over a circle of radius r, denoted by D_0, is obtained from the line integral of v_0 over the circle at range r, divided by the area enclosed by the circle:

$$D_0(r, z) = \frac{1}{\pi r} \sum_i v_0(\phi_i, r, z) \Delta\phi_i$$

$$= \frac{1}{\pi r} \sum_i \int_{-\infty}^{\infty} \int_0^{2\pi} [\eta(\phi_i - \phi', z - z')$$

$$\times v_r(\phi_i - \phi', z - z') W(\phi', z')/B_i'] d\phi' dz' \Delta\phi_i, \quad (5)$$

where $\Delta\phi_i$ is the azimuthal spacing between beam positions at ϕ_i and ϕ_{i+1}.

For clear air echoes, it should be reasonable to assume reflectivity horizontally uniform. Allowing for variation of reflectivity with height and interchanging the order of summation and integration in (5), we obtain

$$D_0(r, z) = \frac{1}{\pi r} \int_{-\infty}^{\infty} \int_0^{2\pi} [\eta(z - z') W(\phi', z')/B'] \times \sum_i v_r(\phi_i - \phi', z - z') \Delta\phi_i d\phi' dz'$$

$$= \int_{-\infty}^{\infty} [\eta(z - z') W_3(z')/B'] \times \left\{ \int_0^{2\pi} W_1(\phi_i) \bar{D}(\phi', r, z - z') d\phi' \right\} dz'. \quad (6)$$

Note that $\bar{D}$ is not available from measurement, rather the divergence $D_0(r, z)$ is obtained from velocities smoothed by the beam function. Since $\bar{D}$ is an average divergence derived from point velocities v_r at finite separation ($\Delta\phi_i$), the value of $\bar{D}$ will change with offset in azimuth (ϕ') due to natural fluctuations in v_r. With infinitely small $\Delta\phi_i$, $\bar{D}$ will exactly equal the true average divergence. Therefore, the beam smoothing in direction ϕ' (horizontal) is desirable to overcome finite sampling of v_r. When $\Delta\phi_i$ is chosen to be less than the antenna beamwidth, and v_r varies linearly within each resolution volume, the inner integral in Eq. (6) closely approximates the true average divergence $\bar{D}(r, z - z')$.

Smoothing in the vertical may still be important since subsynoptic-scale divergence patterns have been observed to have a vertical wavelength comparable to the radars vertical resolution (Rabin and Zrnic', 1980). As a first step, reflectivity is assumed invariate within the vertical beamwidth.[2] Thus, the measured divergence $D_0(r, z)$ can be written simply as

$$D_0(r, z) = \int_{-\infty}^{\infty} \bar{D}(r, z - z') W_3(z') dz'. \quad (7)$$

The purpose of the following few paragraphs is to demonstrate how the actual divergence $\bar{D}(r, z)$ can be retrieved from the radar measured D_0.

The measurements of D_0 are taken on a slant range r which is functionally related to z, the height of the center of the beam. For a Gaussian beam pattern we can write

$$W_3 = (1/\beta\pi) \exp[-(z'/\beta)^2], \quad (8)$$

where $\beta^2 = (r\theta_0)^2/(8 \ln 2)$ with θ_0 the 3 dB beamwidth (see, e.g., Zawadzki, 1973). Eqs. (7) and (8) give

$$D_0 = \frac{1}{\beta\sqrt{\pi}} \int_{-\infty}^{\infty} \bar{D}(r, z - z') \exp[-(z'/\beta)^2] dz'. \quad (9)$$

We now consider a Fourier expansion of $\bar{D}$ at a fixed range r, i.e.,

$$\bar{D} = a_0 + \sum_n (a_n \cos k_n z + b_n \sin k_n z), \quad (10a)$$

which combined with (9) leads to

$$D_0 = a_0' + \sum_n (a_n' \cos k_n z + b_n' \sin k_n z), \quad (10b)$$

where

$$\frac{a_n'}{a_n} = \frac{b_n'}{b_n} = \exp\left[- \frac{(k_n \theta_0 r)^2}{32 \ln 2} \right], \quad (11a)$$

$$k_n = \frac{2\pi n}{H}, \quad (11b)$$

and H is the total depth of measurement. Thus, a vertical profile of average horizontal divergence can, in principle, be deconvolved from the beam pattern. However, the high-frequency Fourier components will be damped by the beam smoothing below the precision of the measurements and therefore become non-retrievable.

We now consider the desirable sampling interval in height such that the maximum of detail can be retrieved from the measurements of D_0. We will refer to the ratio in Eq. (11) as the damping factor A, where

$$A = \exp\left[- \frac{(2\pi n \theta_0 r/H)^2}{32 \ln 2} \right]. \quad (12)$$

At least two points per wavelength are needed to identify a Fourier component (Nyquist frequency). Thus, the highest resolvable wavenumber n_{max} is given by

[2] NSSL radar data indicate a vertical reflectivity change of about 6 dB km^{-1} in the clear planetary boundary layer. A complete treatment of the divergence retrieval requires deconvolution of the vertical reflectivity profile. This is left to a future study.

$$n_{\max} = \frac{H}{2\Delta Z}, \tag{13}$$

where ΔZ is the vertical sampling interval. The maximum damping factor is therefore

$$A_{\max} = \exp\left[-\frac{(\pi\theta_0 r/\Delta Z)^2}{32 \ln 2}\right] \tag{14}$$

or, in terms of the elevation sampling interval $\Delta\theta$,

$$A_{\max} = \exp\left[-\left(\frac{\pi^2}{32 \ln 2}\right)\left(\frac{\theta_0}{\Delta\theta}\right)^2\right]. \tag{15}$$

On the other hand, the uncertainty in measurement of D_0 is given by Rabin and Zrnic' (1980) as

$$\sigma_{D_0} \approx \frac{2}{r}\frac{\sigma_{v_r}}{\sqrt{M}}, \tag{16}$$

where M is the number of independent velocity samples at each elevation ($M \approx 360$) and σ_{v_r} the standard error in velocity estimates (1–2 m s^{-1}); σ_{D_0} appears as noise in the measurements of D_0 and will be amplified if (11) is used for deconvolution. Thus, although (13) indicates that the finer the sampling interval the higher the order of the resolvable Fourier component, the error, after deconvolution, on these components may become intolerable. We assume that the noise is white within the Nyquist interval ($0 \leq n \leq n_{\max}$). The standard error in each wavenumber interval is given by

$$\sigma_n = \frac{\sigma_{D_0}}{n_{\max}\sqrt{2}}, \tag{17}$$

Note that σ_n will be amplified in deconvolution by the inverse of (15) (as a factor) and the error in the deconvolved $n_{\max}$ component, obtained by combining (13), (15), (16) and (17), is

$$\epsilon = \frac{\sigma_n}{A} = \sigma_{v_r}\left[\frac{8\theta_0}{rMH}\left(\frac{\Delta\theta}{\theta_0}\right)\right]^{1/2} \exp\left[\frac{\pi^2}{32 \ln 2}\left(\frac{\theta_0}{\Delta\theta}\right)^2\right]. \tag{18}$$

As an example we take some typical values: $H = 4$ km, $\sigma_{v_r} = 1$ m s^{-1}, $M = 360$, $\theta_0 = 1°$. With these values Fig. 4 is obtained. Thus, at $r = 50$ km, elevation sampling intervals of the order of one-half of a beamwidth will yield divergence measurements which after deconvolution will be affected by errors of the order of 10^{-5} (corresponding to $n_{\max} \sim 5$). This is of the same order of magnitude as the measurement itself and therefore unacceptable. On the other hand, if $\theta_0/\Delta\theta \approx 1$ the error approaches an acceptable level but the retrievable n becomes small, indicating that the divergence measurements can be considered quantitative only if the details of the vertical structure of divergence are of no interest. In other words, we should not expect to retrieve more than a linear trend and a wavenumber

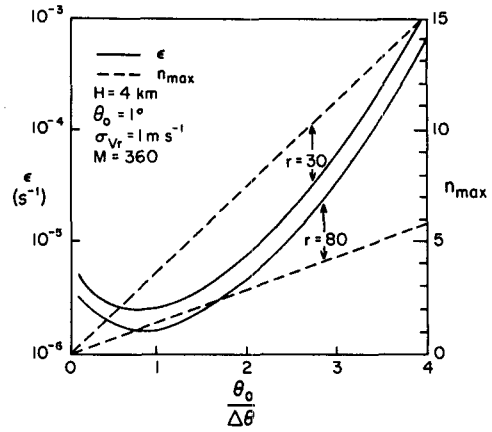

FIG. 4. Highest wavenumber and error in deconvolution as a function of elevation steps within the 3 dB beamwidth.

$n = 2$. However, ϵ can be reduced further by range and/or time averaging. For example, it will require 100 independent measures of D_0 in range to reduce ϵ an order of magnitude. This would allow deconvolution of up to five wavenumbers with $\theta_0/\Delta\theta \approx 2$ (Fig. 4).

The severity of the beam smoothing considered here will depend on the variability of the divergence within the radar beamwidth. As we will see in the next section, the vertical structure of divergence is quite complex and it is likely that some deconvolution of the measurements is necessary in order to obtain quantitative information.

The mathematical analysis of the Doppler radar measured horizontal divergence given here points to the limitations in the quantitative interpretation of the measurements. However, with sufficient data sampling in time and elevation, there is a possibility of reducing the effects of beam smoothing.

5. Data and analysis

Measurements of Doppler velocity in the pre-storm clear air were taken with the NSSL radar located at Norman, Oklahoma on 19 June 1980. The times of observations were 1530, 1600, 1630, 1700 and 1800 CST. Seven antenna elevation angles were used during the measurements: 0.4, 0.8, 1.2, 2.0, 3.0, 4.0 and 5.0°. Sufficient radar signals were available in the lowest 3 km above ground. At distant ranges, only the lowest elevation scans are usable, limiting the number of resolvable wavenumbers to about 2. Nevertheless, an attempt was made to evaluate the importance of the beam smoothing on the determination of the vertical profile of the large-scale divergence.

Fig. 5 shows the range-dependent average divergence, for the seven elevation angles, corresponding to measurements taken at 1630 CST. The 2° elevation curve, for example, has random-like oscillations of D_0 beyond 70 km. These probably indicate uncertainty

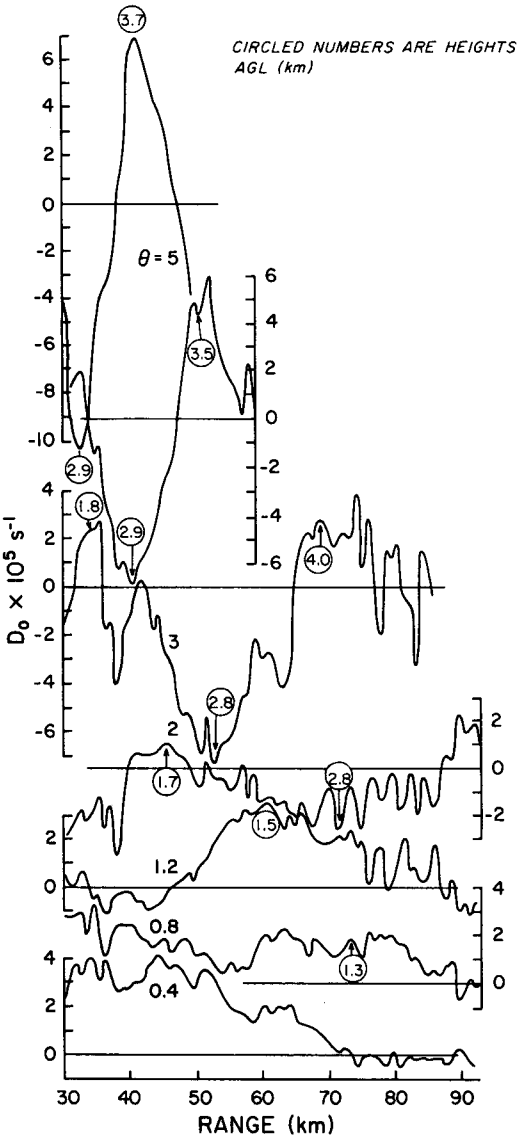

FIG. 5. Single Doppler radar measurements of average horizontal divergence as a function of range and at various antenna elevations.

in the determination of D_0 due to weak radar signals. Nevertheless, a smoothing over a few kilometers in range will yield meaningful information. Therefore, after smoothing the curves of Fig. 5 over 2.5 km in range (five independent measurements), profiles of D_0 vs. height are determined at five ranges (r = 32.6, 37.1, 41.6, 46.1, and 50.6 km) and used in a Fourier analysis. Linear trends from these values of D_0 were removed before three Fourier components were fitted at every range. The profiles of $D_0(r, z)$ obtained in this way are shown in Fig. 6a. With the aid of Eqs. (10) and (11), these profiles were deconvolved and the resulting profiles are shown in Fig. 6b. It is clear that, although the deconvolution results in larger magnitude of divergence, the general shape of the curve is maintained. The same procedure was applied to eight vertical profiles of divergence taken between r = 36 and 77 km. In this case only two Fourier components were determined at each range since the sampling rate at the furthest range does not justify a finer analysis. These profiles were averaged together in order to enhance the accuracy in D_0. The average vertical profiles of divergence before and after deconvolution are shown in Fig. 7. As expected, the effect of deconvolution is more pronounced at these more distant ranges, although it does not change drastically the appearance of the profile.

6. Discussion

The goal of deconvolution is to obtain the most quantitative information possible. However, in this particular case, the measurements of average divergence yield useful qualitative information even when the beam smoothing problem is ignored. Fig. 8 shows a time sequence of vertical profiles of large-scale divergence obtained by a simple range average of all the measurements of D_0 between 30 and 90 km in range. Thunderstorm activity developed about 50 km west of the radar 1¾ hours after the final divergence measurement (1940 CST). These storms gradually increased in size and intensity and reached severe limits. [For a more complete description see: Koscielny *et al.*, (1982).] The time sequence shown in Fig. 8 reveals a marked change to convergence below 2.0 km between 1700 and 1800 CST (the divergence profile at 1730 is from another radar located 40 km to the northwest). As suggested by Rabin and Doviak (1982), the development of low-level convergence appeared important in destabilizing the atmosphere through adiabatic cooling, thus lowering the threshold of vertical uplift necessary for air parcels to reach their level of free convection.

7. Conclusions

Information about convective scales in the pre-storm boundary layer is contained in the radar-measured divergence, but this information is not direct and has to be retrieved through a somewhat involved data analysis. Beam smoothing, reflectivity weighting and the complication introduced by conical scanning of the atmosphere render the raw measurement of divergence qualitative, even if the mean Doppler shift is probably the parameter most reliably determined by a weather radar.

A deconvolution technique is developed and applied. The optimum antenna scanning program for this application is such that successive elevations are separated by about one-half of the 3 dB beamwidth. The divergence profiles are changed only little after deconvolution. Hence, in this case, measurements of average

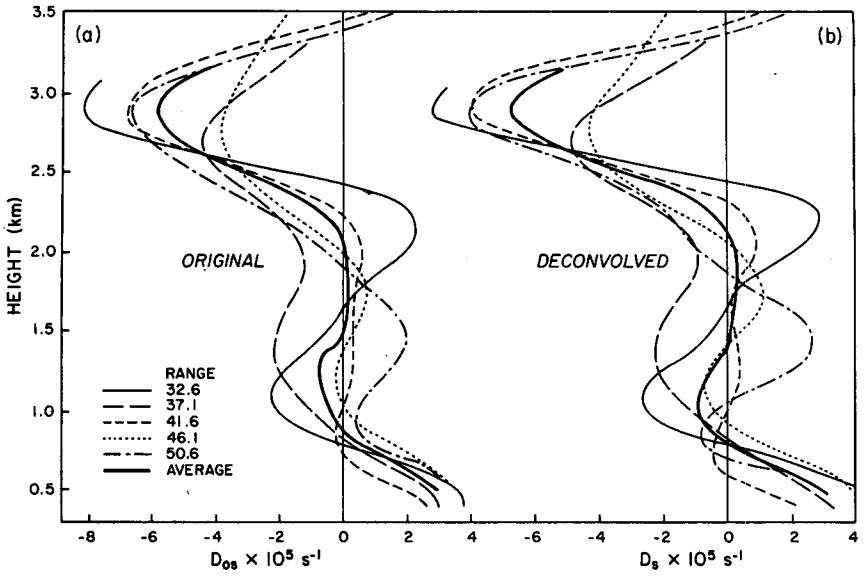

FIG. 6. Three Fourier component approximation to the vertical profile of divergence at various ranges (a) fitted to the measurements in Fig. 5 and (b) after deconvolving the profiles.

horizontal divergence (without correction for beam smoothing) reveal much about the nature of divergence before convection. The Doppler measurements show a rapid change to convergence about 2 h before the formation of thunderstorms. Since the intensity of convergence on the mesoscale is one important factor in forecasting the time of storm development and subsequent precipitation intensity, further efforts to render the measurements of divergence more quantitative are advisable.

Divergence estimates represent the least restrictive VAD derivative. Other parameters such as wind speed, direction and deformation require more restrictive assumptions. The effect of beam smoothing on these VAD derivatives and the scale for which they are representative should be studied.

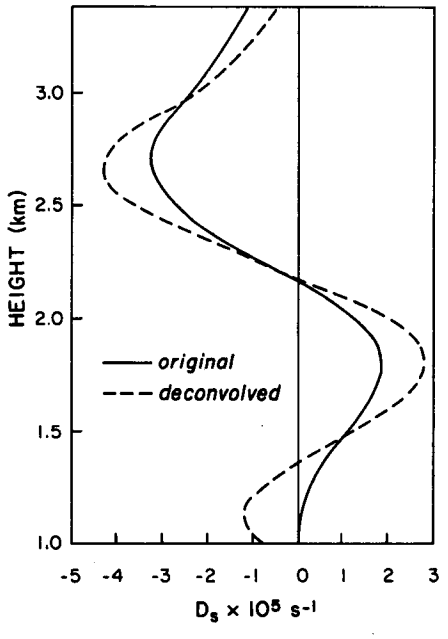

FIG. 7. Two-Fourier component approximation to the divergence profile obtained from range averaging before and after deconvolution.

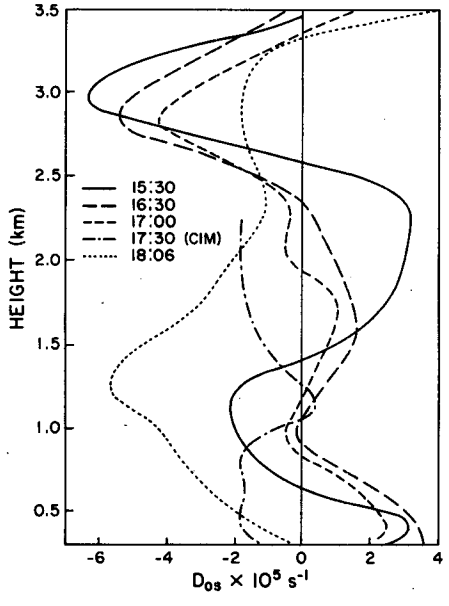

FIG. 8. Time sequence of large-scale vertical profiles of horizontal divergence (beam smoothing effect not compensated). The 1730 CST curve was obtained from data taken by the Cimarron radar operated at elevation angles of 0.4, 0.8 and 1.2°.

Acknowledgments. This work was made possible through NEXRAD (U.S. National Weather Service) Grant NA81AA-D-00020 and CIMMS (University of Oklahoma's Cooperative Institute for Mesoscale Meteorological Studies). Mr. Steven D. Smith was responsible for much of the data processing work. Thanks goes to Drs. Dusan Zrnic', Peter Ray and Richard Doviak for their encouragement and valuable suggestions. Typing was done by Jan Olinghouse, Joy Walton and Michelle Foster. Figures were drafted by Joan Kimpel.

REFERENCES

Browning, R. A., and R. Wexler, 1968: The determination of the kinematic properties of a wind field using Doppler radar. *J. Appl. Meteor.*, **7**, 105–113.

Doviak, R. J., and D. S. Zrnic', 1978: Receiver bandwidth effect on reflectivity and Doppler velocity estimates. *J. Appl. Meteor.*, **18**, 69–76.

Easterbrook, C. C., 1975: Estimating horizontal wind fields by two-dimensional curve fitting of single Doppler radar measurements. *Preprints 16th Radar Meteorology Conf.*, Houston, Amer. Meteor. Soc., 214–219.

Koscielny, A. J., R. J. Doviak and R. M. Rabin, 1982: Statistical considerations in the estimation of divergence from single Doppler radar and application to pre-storm boundary layer observations. *J. Appl. Meteor.* **21**, 197–210.

Rabin, R. M., and R. J. Doviak, 1982: Prestorm observations in the clear air boundary layer with a Doppler radar. *Preprints 12th Conf. Severe Local Storms,* San Antonio, Amer. Meteor. Soc., 425–429.

——, and D. S. Zrnic', 1980: Subsynoptic scale vertical wind revealed by dual-Doppler radar and VAD analysis. *J. Atmos. Sci.*, **37**, 644–654.

Stevens, J. J., 1967: Filtering responses of selected distance-dependent weight functions. *Mon. Wea. Rev.*, **95**, 45–46.

Thomas, G. B., Jr., 1968: *Calculus and Analytic Geometry,* 4th ed. Addison-Wesley, 818 pp.

Ulanski, S. L., and M. Garstang, 1978: The role of surface divergence and vorticity in the life cycle of convective rainfall. Part I: Observation and analysis. *J. Atmos. Sci.*, **35**, 1047–1062.

Waldteufel, R., and H. Corbin, 1979: On the analysis of single Doppler data. *J. Appl. Meteor.*, **18**, 532–542.

Zawadski, I. I., 1973: The loss of information due to finite sample volume in radar-measured reflectivity. *J. Appl. Meteor.*, **12**, 683–687.